PHYSICAL REVIEW B VOLUME 60, NUMBER 4 15 JULY 1999-II

Optical transitions of paramagnetic Ge sites created by x-ray irradiation of oxygen-defect-free Ge-doped SiO_2 by the sol-gel method

N. Chiodini, F. Meinardi, F. Morazzoni, A. Paleari, and R. Scotti
Istituto Nazionale Fisica della Materia, Dipartimento di Scienza dei Materiali, Università di Milano-Bicocca, via Cozzi 53, 20125 Milano, Italy

(Received 9 February 1999)

Optical transitions of radiation-induced paramagnetic Ge centers have been investigated in Ge-doped SiO_2 samples containing a negligible amount of native oxygen coordination defects, whose optical absorption usually dominates the UV spectral range. The analysis of optical and electron paramagnetic resonance (EPR) spectra following different irradiation and thermal annealing treatments shows that two optical absorptions (at 4.4 and 5.7 eV) are related to an orthorhombic EPR signal [Ge(1) signal in literature], while a band at about 6.3 eV follows the evolution of an axial signal [Ge(3) signal] already attributed to axial E'-Ge center. No evidence of another orthorhombic EPR signal observed by other researchers [Ge(2) signal] has been found in our samples. Our results suggest that the previous assignments of the 4.4- and 5.7-eV bands to Ge(1) and Ge(2) centers, respectively, be changed. Instead, both electronic transitions are likely to be ascribed to the sites responsible for the Ge(1) signal. This conclusion has been checked by comparing anisotropy and inhomogeneous dispersion of the principal *g*-tensor values with energy separation and the relative bandwidth and intensity of the optical bands. Structural models of the Ge site responsible for the Ge(1) signal have also been discussed. A structure like the one proposed for the E'_α center is suggested, attributing the orthorhombic distortion to a nearby oxygen excess group. [S0163-1829(99)05128-0]

I. INTRODUCTION

Defects in silicon dioxide are extensively investigated because of their effects on the physical properties of this material, which is widely employed in several technological applications. The E'-Si site, consisting of a threefold coordinated silicon with an unpaired sp^3 electron,[1] is by far the best characterized defect in SiO_2. This is based upon the well grounded correlation between the optical activity and the paramagnetic resonance signal of this defect, established by the early work of Weeks in 1956.[2] The knowledge of the optical transition energy of the E' center together with the local anisotropy and disorder-induced distribution of Hamiltonian parameters obtained from electron paramagnetic resonance (EPR) measurements,[3,4] gives valuable inputs for the assessment of theoretical models of defect structures in the amorphous network of silicon dioxide.[5,6]

Extrinsic variants of the E' defect were also identified in doped silica, with Ge or Sn substituting for silicon.[7,8] In this type of material the E' species are valuable probes of interesting photoactivated effects that can be employed in optoelectronics and fiber optics to generate a refraction index grating.[9–11] Nevertheless, the extrinsic variants of the E' center are less characterized than the Si parent defect, and the effects of the dopant ion on the energy levels of the defect are still to be experimentally defined. Information about the ground state of the Ge variant of E' center comes from the EPR analysis carried out by Friebele, Griscom, and Siegel.[7] By contrast, optical transition energies associated to the E'-Ge centers are a matter of controversy:[12–15] bands at 5.7, 5.9, 6.2, and 6.3 eV were proposed to be correlated with the EPR signal of E'-Ge centers, while bands at about 4.4 and 5.7 eV were correlated to lower-symmetry Ge-related EPR active defects [giving rise to the Ge(1) and Ge(2) signals, respectively].[12] These were initially attributed to orthorhombic variants of the E'-Ge centers[7] but, more recently, to electrons trapped at regular Ge sites.[16–18] In fact, some controversy exists about the structure of the EPR sites with lower symmetry.

Difficulties arise in identifying the optical activity of radiation-induced paramagnetic Ge sites, owing to the presence in Ge-doped SiO_2 of strong and broad absorption bands at about 5.2, 6.5, and 7.3 eV,[13,14,19,20] which usually dominate the investigated spectral region and make it difficult to carry out a spectral analysis on its minor components. These intense bands (mainly due to diamagnetic defects) are related to nonstoichiometry of oxygen and to Ge-doping effects due to different thermochemical equilibrium properties of Ge with respect to Si.[14,21] These bands are always present in Ge-doped SiO_2 produced by high-temperature preparation processes (melting, chemical vapor deposition, and high-temperature sintering of sol-gel material).

We succeeded in synthesizing Ge-doped silicon dioxide with a negligible amount of native oxygen coordination defects. This allowed us to improve the investigation of the optical properties of radiation-induced paramagnetic Ge centers and to correlate them to the peculair features of their EPR spectrum according to a different attribution. As a result of the present study, the interpretation of the paramagnetic features of Ge-related EPR signals is to be reconsidered.

II. EXPERIMENTAL PROCEDURE

Ge-doped silicon dioxide samples (Ge:SiO_2 from 0.1% to 3 weight %) were produced by hydrolysis and condensation of $Si(OC_2H_5)_4$ and $Ge(OC_2H_5)_4$ in an H_2O-ethanol solution by sol-gel method according to the following procedure: 7

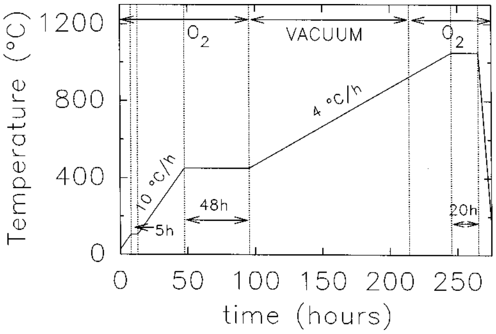

FIG. 1. Heating procedure.

cm^3 of ethanol were mixed with 2.5 cm^3 of $Si(OC_2H_5)_4$ (Stream Chemicals 99.9999%) and with the appropriate $Ge(OC_2H_5)_4$ amount; 1.5 cm^3 of H_2O were then added to the mixture under stirring to obtain a clear solution. The obtained sols were kept at 40 °C until complete gelation [within 3 to 5 days depending on the $Ge(OC_2H_5)_4$ amount] was achieved. Drying to xerogel was obtained in 2 weeks at 40 °C upon solvent evaporation. Xerogels were then treated by thermal process as shown in the diagram in Fig. 1. Plate-shaped samples approximately 1 mm-thick were finally obtained. No further treatment of either cutting or surface polishing was carried out on the materials in order to avoid impurity contamination. Polycondensation and densification of the materials were monitored based upon Raman spectrum changes in the region 200–1200 cm^{-1}. Samples were then x-ray irradiated at room temperature at increasing doses 1.5×10^2 to 3.6×10^3 Gy by an x-ray tube with *W* target at a voltage of 32 kV and a current of 20 mA. Thermal stability of the x-ray-induced optical and EPR spectra was checked one month after irradiation. Isochronal thermal annealing experiments were performed by keeping the samples 5 min at fixed temperatures in air.

EPR measurements were carried out at 300 K by a BRUKER EMX spectrometer operating at *X* band (9.75 GHz). Microwave power values between 0.5 and 200 mW were employed to identify saturation effects. g values were calculated by comparison with a α,α'-diphenyl-β-picryl-hydrazyl standard.

Absorption spectra, between 3.5 and 6.5 eV, were obtained by means of a CARY2300 VARIAN double beam spectrophotometer. The spectral bandwidth was kept to 1 nm. Absorption from atmospheric oxygen was minimized by purging the instrument with a nitrogen flux through monochromator, detector, and sample chambers. Baseline correction for the instrument response was carried out. Effects due to diffuse scattering of light and surface reflection were taken into account by subtracting the spectrum of the unirradiated sample.

III. RESULTS

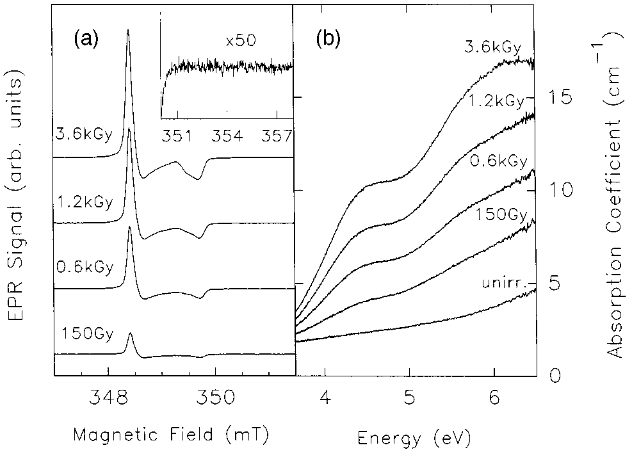

FIG. 2. (a) First derivative EPR spectra (at 300 K) of a Ge-doped SiO_2 sample after x-ray irradiation at the indicated doses. The spectral region corresponding to $g = 1.987$ is shown in the inset, amplified by a factor 50. (b) UV absorption spectra of the same sample before and after x-ray irradiation at the indicated doses.

Before x-ray irradiation, no EPR or optical activity is observed below 6.5 eV. Upon x-ray irradiation at different doses, an orthorhombic EPR signal grows with components at about 348.4, 348.7, and 349.7 mT [Fig. 2(a)]. An optical absorption pattern also arises showing components at about 4.5 eV and around 6 eV, the latter region with a complex structure evidenced by a shoulder just above 5.5 eV superimposed to a band centered at energy values higher than 6 eV [Fig. 2(b)]. The shape of the EPR spectra in Fig. 2(a) reproduces the features of the Ge(1) orthorhombic signal whose g principal values are[7] $g_1 = 2.0007$, $g_2 = 1.9994$, and $g_3 = 1.9930$. Small contribution from the axial Ge(3) variety [$g_{\parallel} = 2.0011$, $g_{\perp} = 1.9945$ (Ref. 7)] may be observed at around 349.5 mT at the highest irradiation doses. Radiation induced absorption after three irradiation steps is reported in Fig. 3, the spectrum of each step being the difference between spectra before and after each irradiation. In the three spectra, the presence of two main components at 4.4 and 5.7 eV and a minor component at higher energy is more evident.

EPR and optical spectra collected 30 days after the latter irradiation are reported in Fig. 4, together with those taken after isochronal thermal annealing at the indicated temperatures. The EPR spectra [Fig. 4(a)] show a decrease in the

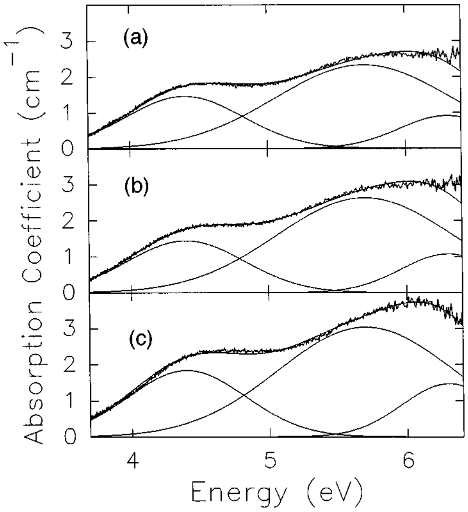

FIG. 3. Radiation-induced absorption (difference between spectra before and after each irradiation) after the second (a) the third (b) and the fourth (c) irradiation step of Fig. 2(b). Numerical fit of the spectra are also reported.

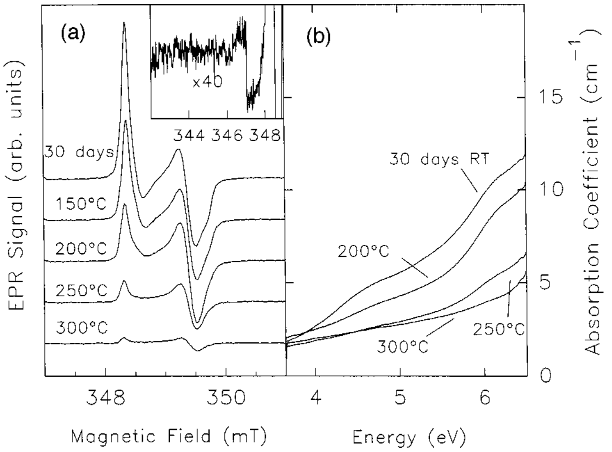

FIG. 4. (a) First derivative EPR spectra (at 300 K) of a x-ray irradiated Ge-doped SiO_2 sample after 30 days at 300 K and subsequent isochronal (5 min) annealing at the indicated temperatures. The spectral region of the nonbridging oxygen hole center signal is shown in the inset, amplified by a factor 40. (b) UV absorption spectra of the same irradiated sample after the same bleaching steps.

amplitude of the main orthorhombic Ge(1) signal while the Ge(3) axial component appears more stable. The Ge(3) component becomes the only detectable signal after annealing at $T \geqslant 250\,°C$, decreasing below the detection limit after treatment at 350 °C. At the same time, the absorption spectrum shows selective bleaching of the radiation-induced pattern [Fig. 4(b)], with a more stable component above 6 eV, almost isolated after annealing at $T \geqslant 250\,°C$. The shape of the absorption spectrum changes slightly by annealing at different temperatures [Fig. 4(b)], the structures at 4.4 and 5.7 eV shifting towards higher energy. This is confirmed by differential spectra (Fig. 5) showing the components bleached after each thermal step at slightly different positions.

The g-value distributions of the orthorhombic Ge(1) and the axial Ge(3) EPR signals, as well as the relative weights of the two signals in the different spectra, are obtained from the numerical fit of the EPR spectra. In Fig. 6 the results of the deconvolutions are shown for a representative situation, i.e., after annealing at 150 °C. Numerical fit is carried out as a weighted sum of powder patterns giving rise to g values distributions for each principal value that account for the site-to-site disorder of the amorphous network.[3] Mean g values and widths of the distributions in Figs. 5(b) and 5(c) are obtained through minimization procedure.[22] No feature in the EPR spectra around $g = 1.987$ suggests any contribution from Ge(2) signal[7] above the detection limit [inset in Fig. 2(a)]. Very weak contributions from nonbridging oxygen hole centers in concentrations of above two orders of magnitude lower than the paramagnetic Ge centers concentration are observed after annealing [inset in Fig. 4(a)].

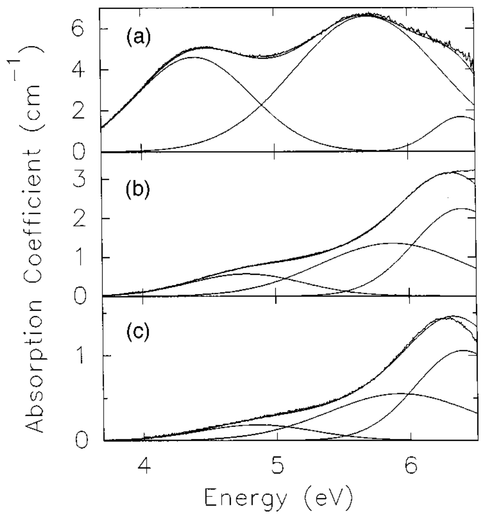

FIG. 5. Bleached absorption (difference between spectra before and after each bleaching step) after 30 days at 300 K (a), 5 min at 200 °C (b), and 5 min at 250 °C (c). Numerical fit of the spectra are also reported.

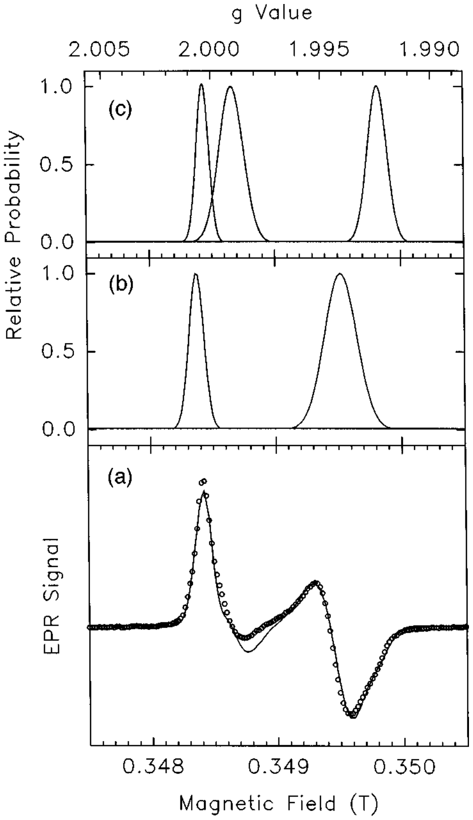

FIG. 6. (a) First derivative EPR spectra (at 300 K) of a Ge-doped SiO_2 sample after x-ray irradiation at a dose of 36 kGy and annealed 5 min at 150 °C (circles), and numerical fit (full line) obtained by a weighted sum of powder patterns of orthorhombic and axial signals (see text). (b) and (c) show the g value distributions used for the numerical fit.

Numerical fits of the optical spectra were also performed. All spectra collected immediately after x-ray irradiation [Fig. 2(b)] can be successfully reproduced as superposition of three bands centered at 4.4, 5.7, and 6.3 eV with bandwidths (full width at half maximum) 0.9, 1.5, and 0.8 eV, respectively. Instead, spectra collected following thermal bleaching cannot be reproduced with exactly the same spectral parameters but require a blueshift from 4.4 to 4.6 eV and from 5.7 to 5.9 eV of the two bands at lower energy. Results of the fit of the radiation-induced absorption and of the bleached spectrum are reported in Figs. 3 and 5. Satisfying fit of spectrum bleached for 30 days at 300 K (Fig. 5) is obtained with parameters used to fit the spectra after x-ray irradiation (Fig. 3). This shows that the main contribution to the radiation-

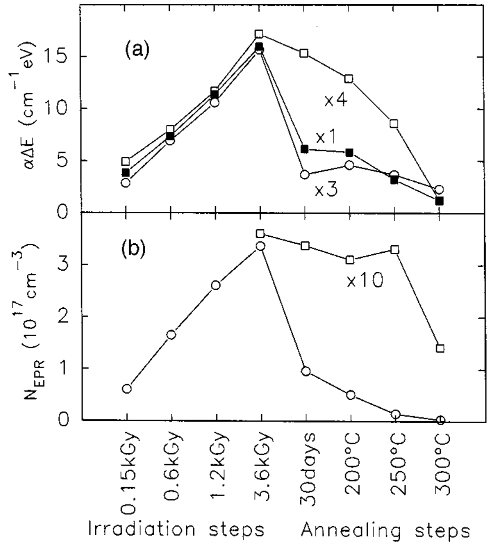

FIG. 7. (a) Product of intensity and bandwidth of the radiation-induced absorption bands centered at 4.4 (○), 5.7 (■), and 6.3 eV (□); (b) concentration of Ge(1) (○) and Ge(3) (□) centers estimated by double integration and numerical analysis of the EPR signal.

induced spectrum (the 4.4- and 5.7-eV bands) is also the less stable one (bleachable at room temperature). Deconvolutions of differential spectra after subsequent thermal bleaching reported in Fig. 4 show the blueshift of the low-energy components. Figure 7(a) summarizes the integrated areas of the optical bands obtained from the deconvolutions of all spectra (in differently irradiated or annealed samples) while Fig. 7(b) shows the double integrated areas of the axial and orthorhombic first derivative EPR signals, after the same treatments, as obtained by the numerical fit. It is worth noting that the areas of the 4.4 and 5.7 eV bands are strongly correlated, maintaining the same ratio within experimental error. Moreover, radiation-induced optically active and paramagnetic species follow quite similar behaviors suggesting the same origin for the 4.4 and 5.7 eV bands and the orthorhombic Ge(1) EPR signal, as well as a similar correlation between the 6.3 eV band and the axial Ge(3) EPR signal.

IV. DISCUSSION

The preparation method we have proposed provides samples with good optical transmission in the UV region and allows us to effectively analyze the optical properties of radiation-induced EPR centers in Ge-doped SiO_2. Indeed, in contrast with observations in Ge-doped SiO_2 prepared by different procedures, the 5.2- and 6.5-eV bands—associated, respectively, to oxygen vacancies and to undefined Ge-doping effects—are completely lacking. We have also avoided Ce^{3+} doping, used by some authors in probe-ion characterization of radiation-induced Ge centers,[18] because the related bands at about 4 and 5 eV can complicate spectral analysis of the optical spectrum. Previous studies were possibly affected by uncertainties deriving from spectral subtraction of other components that can be influenced by irradiation as well. Instead, in our samples, the only effect of x-ray irradiation on the EPR spectrum is the appearance of the Ge(1) and Ge(3) signals, accompanied by the contemporary growth of optical absorption bands at 4.4, 5.7, and 6.3 eV. No trace of Ge(2) signal is observed. In the following sections we first analyze the relationship between optical bands and EPR centers, then we discuss the possible structural models of defects taking into account the present results together with those available from the literature.

A. Optical activity of paramagnetic Ge sites

The correlation in Fig. 7 between the intensities of the 4.4, 5.7, and 6.2 eV absorption bands and the concentration of EPR Ge(n) centers suggests the attribution of the optical bands to electronic transitions of the EPR sites. In particular, the 6.3-eV band appears to be related to the axial Ge(3) signal while both the 4.4- and 5.7-eV bands (characterized by a nearly constant intensity ratio) could be related to orthorhombic Ge(1) sites. The correlation between 6.3 eV band and Ge(3) signal agrees with the previous attributions.[15] Instead, a single band at 4.4–4.6 eV was attributed in the past[12,15] to the presence of the orthorhombic Ge(1) signal, and a component at 5.6–5.7 eV was ascribed to another Ge-related EPR signal with lower symmetry, i.e., the Ge(2) signal.[12] Our data suggest a revision of the association of the Ge(1) signal to the only 4.4-eV band and the assignment of the 5.7-eV band to the Ge(2) signal that is completely lacking in our spectra. Instead, the constant ratio between the intensity of the 4.4- and 5.7-eV bands suggests the attribution of these bands to transitions of the same type of defect, possibly the site responsible for the Ge(1) EPR signal. The experimental intensity ratio $\alpha_{4.4\,\mathrm{eV}}/\alpha_{5.7\,\mathrm{eV}}\approx 0.6$ is roughly consistent with this interpretation since the oscillator strength f of optical transitions with comparable electric dipole matrix elements should scale with transition energy, giving in our case an expected value $\alpha_{4.4\,\mathrm{eV}}/\alpha_{5.7\,\mathrm{eV}}\approx 0.77$.

We have checked this attribution by analyzing the relationship between spectral features of these bands and the g-tensor anisotropy of the Ge(1) signal. The large orthorhombic distortion of the Ge(1) site—reflected in the anisotropy of the g tensor (specifically in the different shift of g_2 and g_3 from the free electron value $g_e = 2.0023$)—indicates a large splitting of the first excited state of the defect site that can result into two distinct optical transition energies.[7] In a first-order approximation, orthorhombic splitting energy can be calculated by relating the principal g values of the EPR signal with the energy level structure of the center according to the following expression:[7,23]

$$g_1 = g_e, \quad g_{2,3} = g_e - k\frac{\lambda}{\Delta \pm \delta/2}, \tag{1}$$

where Δ and δ are the axial and orthorhombic components of the energy splitting between the ground state and the excited levels, λ is the spin-orbit coupling constant, and k a factor of the order of unity. From above expressions (1), we obtain a relation between the orthorhombic g anisotropy $[g_2 - g_3]$ and the expected peak energies $(\Delta - \delta/2)$ and $(\Delta + \delta/2)$, where the Δ and δ values should correspond to the mean energy and energy separation of the absorption bands of the orthorhombic site:

$$\frac{1}{\delta}\left(\Delta + \frac{\delta}{2}\right)\left(\Delta - \frac{\delta}{2}\right) = \frac{k\lambda}{g_2 - g_3}. \tag{2}$$

By inserting $(g_2-g_3)=6.6\times10^{-3}$ from the fit of the Ge(1) EPR signal and taking as λ the free Ge atom value $\lambda=0.11\,\mathrm{eV}$,[23] we obtain (for $k=1$) $k\lambda/(g_2-g_3)=17\,\mathrm{eV}$. This value matches quite well the value $(\Delta-\delta/2)(\Delta+\delta/2)/\delta=19\,\mathrm{eV}$ calculated from the optical transition energies.

Other features of the optical spectrum have been verified to be consistent with the attribution just proposed [between 4.4 and 5.7 eV bands and Ge(1) EPR spectrum], specifically the disorder-induced broadening and the blueshift caused by thermal bleaching.

As regards the optical bandwidths, a relationship between absorption bandwidths $\partial(E_i)$ and disorder distribution $\partial(g)$ of EPR g values can be obtained by differentiating Eq. (1):

$$\partial(E_i)=\frac{E_i^2}{k\lambda}\partial(g), \tag{3}$$

where E_i are the transition energies between the ground and excited states, peaked at $\Delta-\delta/2$ and $\Delta+\delta/2$. From Eq. (3) we obtain $\partial(E_{4.4\,\mathrm{eV}})/\partial(E_{5.7\,\mathrm{eV}})=0.73$—taking $\partial(g_2)=0.0026$ and $\partial(g_3)=0.0021$ from Fig. 5(c)—to be compared with the value 0.67 calculated from the bandwidths $\partial(E_{4.4\,\mathrm{eV}})=1.0$ and $\partial(E_{5.7\,\mathrm{eV}})=1.4\,\mathrm{eV}$ obtained from the optical absorption spectrum.

As regards the blueshift of the 4.4- and 5.7-eV bands, this effect may be interpreted as arising from selective bleaching of optical species belonging to a single type of defect variety with non-null correlation between transition energies and thermal stability. In other words, higher transition energies would pertain to the more stable sites within the orthorhombic variety of radiation-induced Ge defects. Correlation effects on different properties of defects in glasses are to be expected in experiments where defect concentration gets changed.[24] The expected changes of g_2 and g_3 caused by the blueshift of the 4.4- and 5.7-eV optical energies (amounting at about 0.4 and 0.3 eV, respectively, after the final bleaching step) are [from Eq. (1)] 0.10 and 0.06 mT, respectively. These shifts are below uncertainty in numerical analysis of the orthorhombic signal when this is dominated by the axial Ge(3) spectrum.

In summary, the intensity of the 4.4- and 5.7-eV absorption bands is correlated with the amplitude of the Ge(1) EPR signal during irradiation and thermal annealing experiments and, moreover, the expected optical transitions of the orthorhombic EPR sites match the spectral features of the experimental optical spectrum. This supports the attribution of the 4.4- and 5.7-eV absorption bands to transitions of the same orthorhombic Ge site. Our analysis is also consistent with the approach followed by early investigations.[7] Nevertheless, more recent works correlate the 4.4- and 5.7-eV bands to two different defects, specifically those responsible for the Ge(1) and Ge(2) EPR signals,[12] in spite of the fact that reported optical data are quite consistent with our results: the 4.4-eV band was always observed together with a relevant absorption at 5.7 eV, even if the contemporary presence of negative and positive contributions from other bleached and induced bands in the same spectral range gave rise to apparent strong variations of the intensity ratio of the two bands. The contemporary observation of two variants of orthorhombic EPR signals [the Ge(1) and Ge(2) signals] further complicated previous analyses. But, contrary to what is suggested in the works mentioned above, a correlation between the 5.7-eV band and the Ge(2) EPR signal (undetectable in our samples) can be ruled out.

Oscillator strength f of the observed transitions—following the assignment proposed by us—on the basis of the semiquantitative evaluation of the concentration of EPR centers from double integration of the EPR first derivative spectrum can be estimated. The N concentration value at the irradiation doses employed is in the order of $10^{23}\,\mathrm{m}^{-3}$ [Fig. 7(b)] and may be inserted into the Smakula expression:

$$f=\frac{1}{N}\frac{4\pi\varepsilon_0 m_e c}{\pi e^2}\frac{9n}{(n^2+2)^2}\int\alpha(\nu)d\nu, \tag{4}$$

where n is the refraction index and $\alpha(\nu)$ the frequency dependent absorption coefficient, while other symbols are constants with the usual meaning. The integral, extended over the 4.4- and 5.7-eV absorption bands, ranges between 1 and $5\times10^{17}\,\mathrm{m}^{-1}\,\mathrm{s}^{-1}$, while the multiplying constants (except $1/N$) give a factor of about $3\times10^{5}\,\mathrm{m}^{-2}\,\mathrm{s}$. The resulting f values for the absorption transitions of the orthorhombic Ge sites is 0.4 ± 0.05. Analogous estimation of f for the axial Ge site absorbing at 6.3 eV (with a larger uncertainty due to the lower intensity) gives 0.7 ± 0.2, to be compared with the value 0.5 reported by Ref. 15, and the value 0.14 found for the E'-Si optical absorption at 5.8 eV.[2,25]

B. Structural models for the paramagnetic Ge sites

The Ge(1) and Ge(3) EPR signals were initially attributed to Ge variants of E'-like centers with orthorhombic and axial local symmetry, respectively.[7] This early assignment was based on several similarities with the E'-Si signals, as the anisotropy of the g tensor and the anisotropy of the inhomogeneous g distributions, scaled according to the different spin-orbit coupling effects. Later on, different groups agreed with the attribution of the Ge(3) signal to axial E'-Ge sites, whereas an alternative assignment was proposed for the orthorhombic Ge(1) signal from the analysis of the ^{73}Ge hyperfine structure (hfs).[17] This proposal was then apparently supported by probe ion experiments on Ce^{3+} codoped samples.[18] Specifically, the Ge(1) signal was ascribed to electrons trapped in fourfold coordinated Ge sites following two arguments: (a) the s character of the wave function (defined as $s=100|\psi(0)|^2/|\psi(0)|^2_{\mathrm{free}}$) estimated from the hfs splitting ($s=100A_{\mathrm{iso}}/A_s$ with A_{iso} and A_s the isotropic part of the hf coupling tensor and its free atomic value) is larger than 30%, similarly to some amphoteric impurities (as P and As) embedded in silica with coordination order higher than 3 and with electron-trap character;[16,17] (b) the radiation-induced growth of the Ge(1) signal is favored in Ce^{3+}-doped samples, consistently with the attribution to trap sites for the electrons released from Ce^{3+} ions during irradiation (probe ion experiments[18]).

Here, on the basis of two experimental facts, we reconsider the early attribution of the Ge(1) signal to a low-symmetry variant of E'-Ge center. In fact: (A) a low-symmetry variant of E'-Si signal (the E'_α signal[3]) was observed in pure silica with nearly the same orthorhombic character and without any evidence attributing this to electron trapping in fourfold coordinated Si sites;[3] (B) the difference between the *s* character of the Ge(1) site and the E'-Ge center is smaller than the difference of *s* character of the E'-Ge with respect to the E'-Si.

Point (A) refers to a variant of E'-Si signal analyzed by Griscom[3] and characterized by *g* values 2.0017, 2.0012, and 1.9998. The orthorhombic parameter $[g_2 - g_3] = 1.4 \times 10^{-3}$ is surprisingly consistent with that of the Ge(1) signal ($\approx 7 \times 10^{-3}$) once we take into account the ratio $\lambda(\mathrm{Ge})/\lambda(\mathrm{Si}) \approx 6$ of the spin-orbit coupling constants of the extrinsic and intrinsic defects. Orthorhombic distortion of the E'_α center was tentatively attributed to a neighbor peroxy group formed by the interstitial oxygen atom removed from the Si-O bond during the defect creation from a regular site. So the lower symmetry of this variant, relatively unstable, would depend on the fact that this is not originated by the typical E' precursor, that is the neutral oxygen vacancy, which instead gives rise to a nearly axial defect site. It is remarkable that the Ge(1) signal is dominant in our samples where the oxygen vacancy content is very low (that is the axial E' precursor content) whereas the Ge(3) signal predominates in samples where the 5-eV band is intense (high oxygen deficient center content).[9,10,15,18]

As regards point (B), we have considered all the factors, other than the previously proposed change of coordination order, potentially affecting the *s* character of the wave function of E'-like sites in SiO_2. The normalized spin-density values on *s* orbital of Ge(1) and E'-Ge center (0.35 and 0.30, respectively, corresponding to 35% and 30% of *s* character),[16,17] compared with the 0.24 E'-Si value,[3] indicate that Ge substitution itself is probably the main cause of these differences. In fact, the expected longer Ge-O bond with respect to the Si-O bond (on the basis of both numerical simulations and comparison with the GeO_2 structure) implies lower covalence and a higher spin density on the Ge nucleus at fixed hybridization, thus passing from the E'-Si to the E'-Ge geometry. So, a small change of geometry at fixed coordination order can reasonably justify a change of 25% of the spin density at the nucleus (from 0.24 in E'-Si to 0.30 in E'-Ge). This, in turn, suggests a careful check on the possible effects of the distortion related to the orthorhombic symmetry of the Ge(1) signal. Orthorhombic distortion may be the cause of the higher *s* character of the Ge(1) site with respect to the E'-Ge center, the difference amounting to only 17% of the E'-Ge value. We remark, by contrast, that typical examples of paramagnetic centers on amphoteric impurities in SiO_2 (As and P) show changes of 32% and 43% (respectively) of the *s* character of the unpaired spin by changing from three- to fourfold coordination. Distortion of the E'-Ge site can roughly be quantified, which would justify the different hfs splitting of the Ge(1) signal. The pseudotetrahedral α angle O-Ge-e^- (i.e., the angle formed by a Ge-O bond and the dangling bond of the E' structure) is related to the hfs splitting through a simple relation (well describing the ^{29}Si hfs line shape of the E'-Si signal in pure SiO_2 in terms of dispersion of O-Si-O angles in the amorphous network):[3]

$$\tan \alpha = -\left[2 \left(1 + \frac{c_p^2}{c_s^2} \right) \right]^{1/2}, \qquad (5)$$

where $c_s^2 = A_{\mathrm{iso}}/A_s$ and $c_p^2 = A_{\mathrm{aniso}}/A_p$. Thus, from the values $A_{\mathrm{iso}} = 25\,(29)$ mT and $A_{\mathrm{iso}} = 0.9\,(0.4)$ mT for the E'-Ge [Ge(1)] signal, and taking $|A_s| = 84$ mT and $|A_p| = 4.3$ mT,[26] we would obtain a change of the tetrahedral angle of about 3.5°, from the axial E'-Ge structure to the distorted E' structure possibly responsible for the Ge(1) signal. This distortion is not unreasonable since the disorder-induced distribution of α bond angles in the amorphous SiO_2 network implies by itself a spread of about 1.5° at half maximum of the probability function of the tetrahedral angle,[3] and even more spreaded values in GeO_2 where $106° < \alpha < 113°$ in the quartzlike crystalline form.[27] Therefore a typical source of disorder of the amorphous network, such as a peroxide group, can probably cause such a distortion, lowering the local symmetry from axial to orthorhombic and slightly modifying the ^{73}Ge hfs splitting.

Probe-ion experiments, which were interpreted as suggesting the electron-trap character of the Ge(1) sites, deserve a final comment. The observation of a specific relation between the growth of the concentration of a defect species and the radiation-induced release of electrons from Ce^{3+} ions should only indicate that an electron-trapping process takes part at some stage of defect creation, not necessarily a direct trapping activity in the defect site. In fact, defect creation processes often involve photolytic or radiolytic reactions that give rise to defect pairs (typically Frenkel pairs with oxygen vacancies and oxygen excess sites) or even more complex cascade reactions (sometimes limited by diffusion of some ionic or molecular species). Therefore, electron trapping may occur in any products of the reaction, not necessarily by inducing paramagnetism or optical activity but also by hiding them through saturation of broken and dangling bonds. So, ion-probe experiments may be useful to differentiate distinct creation processes of the same defect species, not to discriminate different defect configurations by supposing only one formation process. An example of this comes from the same probe-ion experiments quoted above[18] that indicated the existence of two indistinguishable variants of E'-Ge center with different thermal stability, identified as arising from electron and hole trapping, respectively.

V. CONCLUSIONS

The synthesis of Ge doped silicon dioxide with a very low content of oxygen vacancy defects allowed us to reconsider the identification of the optical activity of radiation-induced paramagnetic Ge centers and to clarify a few controversies about the local configuration of these sites. As a result of the analysis of optical and EPR spectra after different irradiation and thermal annealing of samples obtained by sol-gel procedure, two absorption components at 4.4 and 5.7 eV appear correlated with the orthorhombic Ge(1) EPR signal, while a band at about 6.3 eV follows the evolution of the axial Ge(3) signal. No trace of Ge(2) EPR signal, previously related to the 5.7-eV absorption, is detected in our samples. Therefore, previous assignments are to be modified by ascribing the 4.4- and 5.7-eV electronic transitions to the site responsible for the Ge(1) signal. This proposal has been verified by comparing the anisotropy and inhomogeneous dispersion of the principal values of the *g* tensor with energy separation and the relative bandwidth and intensity values of the optical bands.

The defect model of the paramagnetic Ge site responsible for the Ge(1) signal has then been reconsidered in the light of our results obtained in a peculiar situation of Ge-doped SiO_2 where oxygen vacancies are not the majority precursors of E' centers. So, radiolytic mechanisms whereby an oxygen atom is moved from its regular site to a nearby position may be dominant during irradiation. This situation resembles the mechanism postulated for the formation of an E'_α center in x-ray irradiated pure silica. E'_α and Ge(1) signals show indeed similar spectral features, creation properties, and thermal stability, suggesting an E'_α-like defect structure for the Ge(1) site, with the orthorhombic distortion due to nearby interstitial oxygen atoms.

ACKNOWLEDGMENTS

The authors gratefully acknowledge valuable discussions with G. Spinolo and L. Skuja, and the technical assistance granted by A. Lazzarini. This work was carried out within a project supported by MURST of the Italian government.

---

[1] F. J. Feigl, W. B. Fowler, and K. L. Yip, Solid State Commun. **14**, 225 (1974).

[2] R. A. Weeks, J. Appl. Phys. **27**, 1376 (1956).

[3] D. L. Griscom, Nucl. Instrum. Methods Phys. Res. B **1**, 481 (1984).

[4] D. L. Griscom, Phys. Rev. B **22**, 4192 (1980).

[5] G. Pacchioni, G. Ieranò, and A. M. Márquez, Phys. Rev. Lett. **81**, 377 (1998).

[6] G. Pacchioni and G. Ieranò, Phys. Rev. B **57**, 818 (1998).

[7] E. J. Friebele, D. L. Griscom, and G. H. Siegel, Jr., J. Appl. Phys. **45**, 3424 (1974).

[8] N. Chiodini, F. Meinardi, F. Morazzoni, A. Paleari, R. Scotti, and G. Spinolo, Phys. Rev. B **58**, 9615 (1998).

[9] H. Hosono, K. Kawamura, N. Ueda, H. Kawazoe, S. Fujitsu, and N. Matsunami, J. Phys.: Condens. Matter **7**, L343 (1995).

[10] T. E. Tsai, C. G. Askins, and E. J. Friebele, Appl. Phys. Lett. **61**, 390 (1992).

[11] B. Poumellec and F. Kherbouche, J. Phys. III **6**, 1595 (1996).

[12] V. B. Neustruev, J. Phys.: Condens. Matter **6**, 6901 (1994).

[13] B. Crivelli, M. Martini, F. Meinardi, A. Paleari, and G. Spinolo, Phys. Rev. B **54**, 16 637 (1996).

[14] H. Hosono, Y. Abe, D. L. Kinser, R. A. Weeks, K. Muta, and H. Kawazoe, Phys. Rev. B **46**, 11 445 (1992).

[15] H. Hosono, M. Mizuguchi, H. Kawazoe, and J. Nishii, Jpn. J. Appl. Phys., Part 2 **35**, L234 (1996).

[16] H. Kawazoe, J. Non-Cryst. Solids **71**, 231 (1985).

[17] Y. Watanabe, H. Kawazoe, K. Shibuya, and K. Muta, Jpn. J. Appl. Phys., Part 1 **25**, 425 (1986).

[18] E. V. Anoikin, A. N. Guryanov, D. D. Gusovsky, E. M. Dianov, V. M. Mashinsky, S. I. Miroshnichenko, V. B. Neustruev, V. A. Tikhomirov, and Yu. B. Zverev, Nucl. Instrum. Methods Phys. Res. B **65**, 392 (1992).

[19] M. J. Yuen, Appl. Opt. **21**, 136 (1982).

[20] M. Gallagher and U. Osterberg, J. Appl. Phys. **74**, 2771 (1993).

[21] M. Martini, F. Meinardi, A. Paleari, L. Portinari, and G. Spinolo, J. Non-Cryst. Solids **216**, 26 (1997).

[22] F. James, *MINUIT—Function Minimization and Error Analysis* (CERN, Geneva, Switzerland, 1994).

[23] F. J. Feigl and J. H. Anderson, J. Phys. Chem. Solids **31**, 575 (1970).

[24] L. Skuja, J. Non-Cryst. Solids **239**, 16 (1998).

[25] D. L. Griscom, J. Ceram. Soc. Jpn. **99**, 899 (1991).

[26] J. R. Morton and K. F. Preston, J. Magn. Reson. **30**, 577 (1978).

[27] E. F. Riebling, J. Am. Ceram. Soc. **51**, 406 (1968).